

Elastic properties of SiO₂ nanostructure in high-pressure conditions

Z. Radi^{a,b,*}, S. Tlili^c, K. Layadi^a, L. Louail^b, A. Yells-Chaouche^a, Y. Madhekour^b, S. Guettouche^a.

^a *Astronomy, Astrophysics and Geophysics Research Center, Algeria.*

^b *Laboratory for Studies of Surfaces and Interfaces of Solid Materials (LESIMS), Ferhat Abbas University, Sétif, Algeria.*

^c *Development of New and Renewable Energies in Arid and Saharan Zones Laboratory (LARENZA), Department of Physics, Faculty of Mathematics and Material Sciences, Kasdi Merbah Ouargla University, Ouargla 30000, Algeria*

In this study, the elastic properties of two high-pressure polymorphs SiO₂ nanostructure, stishovite and CaCl₂-type, are obtained using Density Functional Theory in 0-80 GPa high pressure domain at zero temperature, based on reducing an interacting many-electron problem to a single-electron problem. It is shown that below 40 GPa, the stishovite phase is more stable; superior to this limit, the CaCl₂-type phase becomes more stable, using Gibbs free energy method. Furthermore, the pressure dependence of the density, volume, bulk, and shear moduli were defined in the selected pressure domain.

(Received November 9, 2022; Accepted February 21, 2023)

Keywords: Elastic properties, Stishovite, CaCl₂-type, SiO₂ nanostructure, Density functional theory, High-pressure

1. Introduction

Silicon (Si) and Oxygen (O) are the two most common chemical elements in the earth's crust and mantle. Therefore, it is not surprising that a group of minerals composed basically of these two elements with a number of other ions and named silica, SiO₂, takes on several structural arrangements (SiO₂ is considered the most chemical element in the primitive mantle or bulk silicate Earth; composition, 46 wt %, from [1]). High pressure and temperature have a great role in the stability of the elastic properties of the major materials of the earth's mantle. The high-pressure behavior of these properties can be determined by theoretical methods with certain limitations. There are six different crystalline forms of transformation depending on the pressure ranging from 0 to 300 GPa: quartz, coesite, stishovite, CaCl₂-type, seifertite (α -PbO₂-type), and pyrite [2]. According to [3], the Earth's crust [2] upper mantle is mainly composed of SiO₂, coming from rocks of the Earth's surface sinking into the lower mantle. This mineral is minor in extraterrestrial materials [4].

To understand the phase transitions between the different forms, theoretical and experimental investigations in mantle conditions (principally high pressure) have been developed, especially after the discovery of stishovite by [5] and [6] (stishovite is an honor name from Stishov of the new SiO₂ high-pressure polymorph at pressure to be above 16 GPa and 1200–1400 °C, proposed by [5], who, according to them, they were the first who discovered it in the Coconino Sandstone of the Meteor Crater, Arizona, as a result of a meteoritic impact). According to [6], the stishovite was synthesized first at Okayama University (Japan) using a uniaxial split-sphere type high-pressure apparatus under experimental conditions of 10 GPa and 1000 °C for 30 min, in which the SiO₂ (quartz) was inserted into a graphite heater, pulverized, and examined by X-ray diffraction and microscopic observation. [7] found that stishovite is one of the most anisotropic silicates at the 47 GPa transition point (transition from the stishovite to the orthorhombic CaCl₂-type phase). Previous studies based on thermo-chemical calculations and well summarized in [6],

* Corresponding author: z.radi@craag.dz

<https://doi.org/10.15251/DJNB.2023.181.263>

the boundary curve of the coesite-stishovite transition from the P-t diagram showed that the pressure has not been strongly influenced by the temperature. Also, [8] illustrated the P-t diagram of the stishovite-CaCl₂ transition and showed that it depends mostly on the pressure rather than the temperature (from 227 to 3700 °C temperature variation, the pressure increased only between 60 and 70 GPa). [9] studied the physical properties (elastic modulus, Bulk modulus...) of the major earth's mantle, considering the pressure dependence (from 0 to 140 GPa).

Post-stishovite phases were identified after ~30 years from the discovery of stishovite by [8] and [9], and they are CaCl₂ structure occurring at ~50 GPa and seifertite which occurs at ~100 GPa ([7]) and pyrite structure (occurs above 150 GPa according to [8]). The comparison between experimental results on silica transition phases are controversy. According to [9], the theoretical calculation provides the ideal complement to the laboratory approach and the contact between them is essential. In the present study, based on the Density Functional Theory (DFT), the pressure dependence of elastic stiffness coefficients are computed for the two high-pressure polymorphs of silica, stishovite, and CaCl₂-type, from 0 to 80 GPa at zero temperature. The obtained results are compared to previous studies based on experimental and theoretical investigations, in order to get a level of similitude and/or differentiability, principally from review studies such [9], [10], and [11].

2. Method of elastic properties computation

To compute the elastic properties of stishovite and CaCl₂-type, we used DFT within the generalized gradient approximations from the first principles methods developed by [12], which allows us to reduce an interacting many-electron problem to a single-electron problem ([9]). In this theory, it is proposed that the ground state total energy E of an electronic system can be expressed as a function of its charge density, $n(r)$:

$$E[n(r)] = F[n(r)] + \int V_{ion}(r)n(r)dr \quad (1)$$

where $F[n(r)]$ is a functional contains the electronic kinetic, Hartree and exchange-correlation energies (more details are given in [13]). V_{ion} is Coulomb potential.

In our application of DFT, the Cambridge Serial Total Energy Package (CASTEP) code is used ([14, 15]). It can give information on the total energies, and forces, and insists on an atomic system, as well as the calculation of optimal geometries, band structures, optical spectra... We used the pseudo-potential approximation, plane wave function, and the Monkhorst-Pack scheme to reduce the number of variables and sample the irreducible Brillouin zone ([16]). In the present study, we took a Brillouin zone at the special k-points generated by a sampling grid of 8x8x8 and a wave plane energy cut-off equal to 450 eV, to obtain a good convergence of the calculations for reliable results. The fully optimized structure of stishovite and CaCl₂-type phases of silica was used to determine the elastic proprieties, which allows refining the geometry of a 3D periodic system to obtain a stable structure or polymorph. Pressure dependence of the volume, density, elastic constants were given as curves with some fundamental formulas.

3. Results and discussion

3.1. Phase Transition

The value of the Gibbs free energy (G) is an important parameter for the stability of each possible structural phase, which is given by the relation n° 2.

$$G = E_{tot} + P * V + S * T \quad (2)$$

where: E_{tot} is the total energy; P is the pressure; V is the volume; S is the entropy; T is the temperature. [10] used the Gibbs free energy to determine the phase transition of stishovite-CaCl₂-type in P-t diagram where the Clapeyron slope is 5 ± 1.3 MPa/K.

In this study, we used theoretical calculations for $T = 0$ K, so $G = E_{tot} + P * V$. The enthalpy of formation of each structure (stishovite or CaCl_2 -type phase) was calculated for several pressure values (Figure 1). At each pressure, the stishovite's enthalpy value is taken as the reference and the difference between both phases is presented as the value of the enthalpy of formation of the second phase. This method was used by [17]. Figure 1 shows the enthalpy difference results in the pressure range 10 up to 80 GPa for stishovite and CaCl_2 -type phases. For the last pole, the enthalpy difference variation is influenced by the pressure, with a variety of negative slopes ($\sim -5\text{E-6}$ Atom/eV).

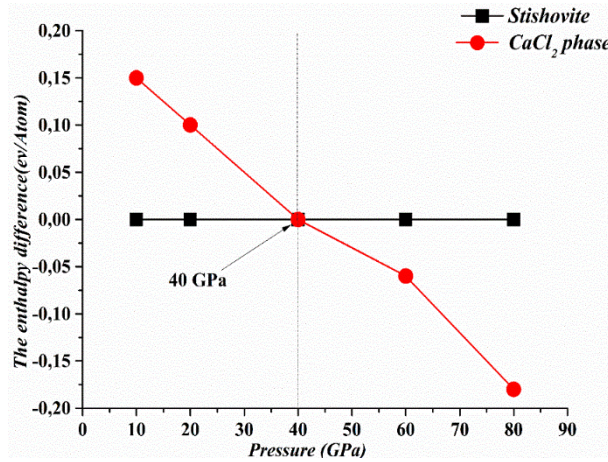


Fig. 1. The variation of enthalpy difference as a function of pressure of stishovite and CaCl_2 -type phases.

The difference in the enthalpy of formation of CaCl_2 -type of SiO_2 decreases with the increasing pressure until it cancels out around a pressure of 40 GPa. This is the phase transition pressure of stishovite. Our results are in agreement with those of [7] (~ 47 GPa), by Raman spectroscopic observations of [18] (49-50 GPa) and [11] (~ 60 GPa), 53.4 GPa by [19]. From this comparison, it is clear that our obtained result of phase transition pressure is smaller.

3.2. Structural properties

The theoretical Equation of State, EoS, which describes the dependence of the cell volume on the external hydrostatic pressure and used in this study for CASTEP is given in the following formulas:

$$P = \frac{3}{2}B \left[\left(\frac{V_0}{V} \right)^{7/3} - \left(\frac{V_0}{V} \right)^{5/3} \right] \times \left\{ 1 + \frac{3}{4}(4 - B') \left[\left(\frac{V_0}{V} \right)^{2/3} - 1 \right] \right\} \quad (3)$$

where B is the bulk modulus and $B' = dB/dP$ its pressure derivative; V is the cell or elementary molecular volume; V_0 is the equilibrium volume

The analysis of P-V is plotted in Figure 2 as V/V_0 ratio variation in the 0-80 GPa domain. The illustration in this figure shows a slowly decreasing as the pressure increases, with a negative slope ($\sim -2.12\text{E-3}$). We compare our obtained results with those of [17] and [19] defined experimentally. We notice that the results are very close for pressures less than 40 GPa, particularly for [17]. Above this limit, the stishovite- CaCl_2 -type phase transition, a clear difference between our result and the experimental results of [19], can be explained by the temperature and pressure conditions ($T = 0$ K, hydrostatic pressure for our calculation; $T = 300$ K, non-hydrostatic pressure for their experiments). The V/V_0 ratio decreases from 1 to 0.89 in the first phase and from 0.89 to 0.823 in the second phase. [20] analyzed the volume variation behavior with temperature and pressure using X-ray diffraction, and they found that for the same pressure, when the temperature increases, the volume becomes important.

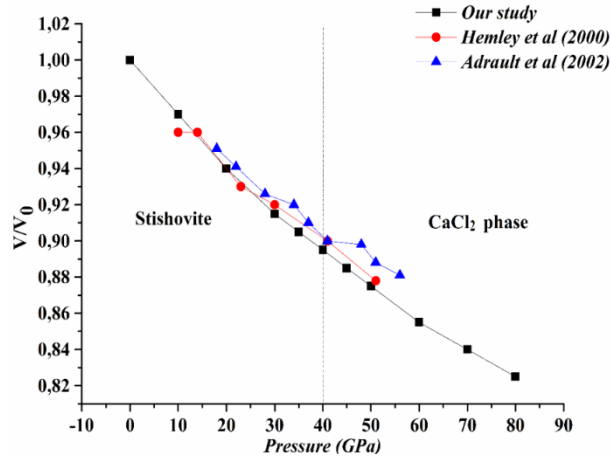


Fig. 2. The V/V_0 as a function of pressure obtained in this study and compared to the experimental results of [17] and [21].

In the present analysis, the pressure dependence of the density, ρ , is plotted in Figure 3 compared to the values from [22], [10], [23] and [24] using the following relationship between the elementary molecule mass (m) and volume (V):

$$\rho = m/V = Z * M/N * V \quad (4)$$

where M is the molar mass; Z is the number of molecules in the elementary molecule; N is the Avogadro number.

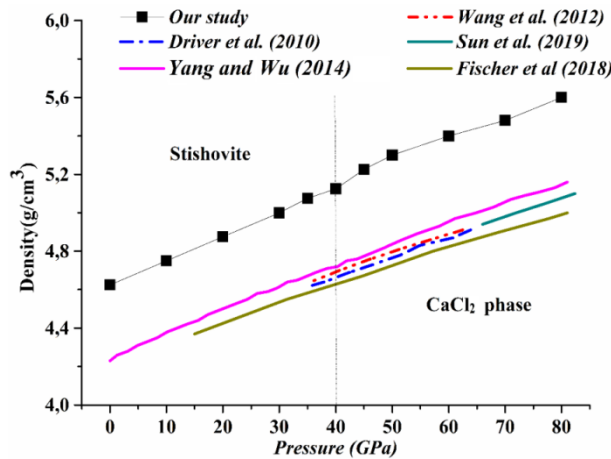


Fig. 3. The variation of density as a function of pressure obtained in this study compared to the densities from [20], [25], [10] [23] and [24].

Our results show that the density of stishovite and CaCl_2 -type increases linearly with pressure, with an average slope of 0.13 and 0.10, respectively. Compared with the previous studies mentioned above and in Figure 3, the density variation obtained in this study is almost parallel, where our calculated values are larger (Figure 3). This difference can be explained by the difference in initial conditions for computation and measurement. [20] compared their obtained results of ρ - P relation with the Primitive Reference Earth Model (PREM), where they considered different temperatures associated with slabs and mantle geotherm, and after 25 GPa, all relations become close with a significant intersection at 65 GPa which corresponds to 1600 km. This confirms that our two studied poles exist in the lower mantle, and their fraction increases with depth ([26]).

3.3. Elastic coefficients

To calculate the elastic constants, C_{ijkl} a strain-stress approach was used in the CASTEP code. This method is based on a set of finite homogeneous deformations that are accompanied by stress according to Hook's law [27]:

$$\sigma_{ij} = C_{ijkl}e_{kl} \quad (5)$$

where σ_{ij} and e_{kl} are stress and strain tensors.

At low pressure, stishovite takes the tetragonal structure with six nonzero elastic constants while in the orthorhombic phase of CaCl_2 -type there are nine nonzero constants. We focus our study on the three values C_{11} , C_{12} , and C_{44} since the other constants increase in the same way in both phases. The pressure dependence of the elastic constants, C_{11} , C_{12} , and C_{44} of stishovite and CaCl_2 -type high-pressure polymorphs is calculated and plotted in Figures 4, 5, and 6. In the stishovite phase, C_{11} increases slowly with the pressure until 35 GPa then it decreases. The same behavior was observed by [5] and [10].

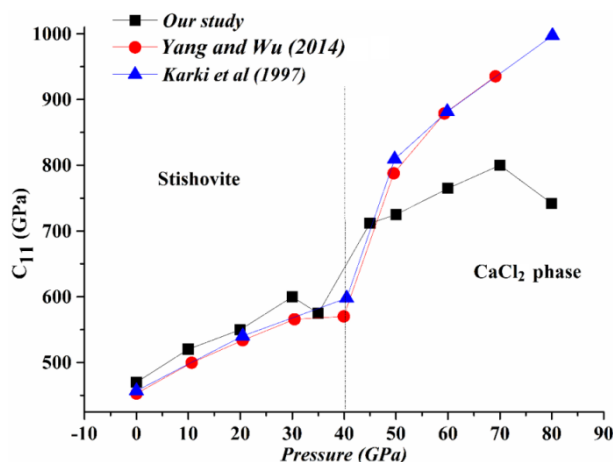


Fig. 4. The variation of elastic constants C_{11} as a function of pressure for stishovite (0 to 40 GPa) and CaCl_2 -type (40 to 80 GPa) compared to [7] and [10].

There is a compression along the X axis. After the phase transition, at 45 GPa in the CaCl_2 -type phase, significant divergence between our result and those of [7] and [10], where our C_{11} increases slowly and falls at 75 GPa which can be related to the CaCl_2 -type-seifertite phase transition. The same variation occurred for C_{22} because in the tetragonal structure $C_{11} = C_{22}$. In the stishovite phase, we observe a faster increase of our far-diagonal C_{12} constant between 30 and 35 GPa due to the phase transition compared to the results of [7] and [10] (Figure 5).

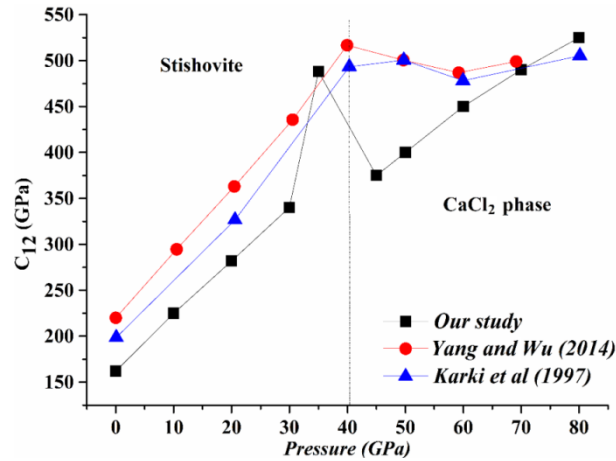


Fig. 5. The variation of elastic constants C_{12} as a function of pressure for stishovite (0 to 40 GPa) and CaCl_2 -type (40 to 80 GPa) compared to [7] and [10].

Between 35 to 45 GPa, the C_{12} decrease dramatically then it resumes the increase as the compared results. In Figure 6, the value of the shear constant C_{44} increases linearly, with a very small slope in the whole pressure interval. This indicates that the main axes keep the same directions.

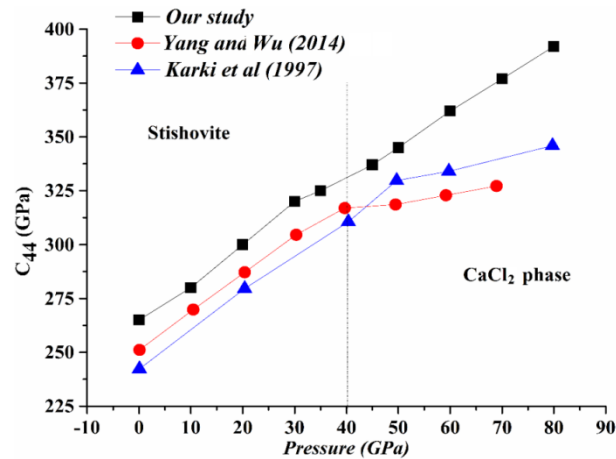


Fig. 6. The variation of elastic constants C_{44} as a function of pressure for stishovite (0 to 40 GPa) and CaCl_2 -type (40 to 80 GPa) compared to [7] and [10].

The values of the elastic constants of stishovite at 0 GPa pressure are in good agreement with many previous studies ([14, 27, 28]) summarized by [9] and [11] presented in Table 1. The values of [29] present a large difference between our results and the previous studies especially for C_{11} , C_{33} and C_{12} (Table 1).

Table 1. Values of the elastic constants (in GPa) of the stishovite phase at 0 GPa.

	C ₁₁	C ₃₃	C ₄₄	C ₆₆	C ₁₂	C ₁₃
GGA (this study)	456	792	265	323	158	177
PWPP ^[11]	456	807	254	325	216	195
LAPW ^[15]	452	776			242	221
PIB ^[17]	623	977	347	424	450	146
Exp ^[16]	453	776	252	302	211	203
BKS potential ^[23]	703	1072	287	260	314	281
ab initio, LDA-PWPP ^[24]	480	735	260	340	245	220
KA pseudopotential ^[26]	~448	776	252	302	211	203
FHI pseudopotential ^[26]	~449	752	~257	323	211	191

GGA: generalized gradient approximation; PWPP: plane wave pseudopotential; LAPW: linearized augmented plane wave; PIB: potential induced breathing; EXP experimental; Beest, Kramer and van Santen: BKS; LDA: local-density approximation; KA and FHI are Troullier-Martins type pseudopotentials

The bulk modulus, B , represents the resistance of the crystal during the application of the constraints, to preserve its volume, whereas the shear modulus, G , which represents the resistance to plastic deformation. To deduce the polycrystalline properties of the material under consideration, it is necessary to average, which is directly related to the wave propagation velocity. Different assumptions were used in [29]:

- Voigt's hypothesis [30]: the continuity of the deformations is assumed, i.e. the grains fit perfectly together but stress discontinuities can appear at the interfaces.
- The Reuss's hypothesis [31]: we assume the continuity of the strains, i.e. that the strains are uniform throughout the aggregate but that the grains do not fit together perfectly.
- Hill's hypothesis: a simple geometric mean of quantities calculated in the Reuss and Voigt cases:

$$G_H = (G_R + G_V)/2 \quad (6)$$

The experiment shows that the numerical results obtained by the Hill's hypothesis are generally not far from the experimental values. For tetragonal symmetry (P42/mnm), the shear modulus according to Voigt's hypothesis [32] is:

$$G_V = \frac{1}{5} \left(\frac{C_{11} + C_{12} - 2C_{13} + 2C_{33}}{6} + \frac{C_{11} - C_{12}}{2} + 2C_{44} + C_{66} \right) \quad (7)$$

The shear modulus according to Reuss's hypothesis ([19]) is:

$$G_R = \left[\frac{1}{5} \left(\frac{6[(C_{11} + C_{12}) + 4C_{13} + C_{33}]}{(C_{11} + C_{12})C_{33} - 2C_{13}^2} + \frac{1}{C_{11} + C_{12}} + \frac{1}{C_{44}} + \frac{1}{C_{66}} \right) \right]^{-1} \quad (8)$$

For orthorhombic symmetry, the shear modulus according to Voigt hypothesis ([31]) is:

$$G_V = \frac{1}{15} (C_{11} + C_{22} + C_{33} - C_{12} - C_{13} - C_{23}) + \frac{1}{5} (C_{44} + C_{55} + C_{66}) \quad (9)$$

The shear modulus according to Reuss's hypothesis ([32]) is:

$$G_R = \frac{15}{4(S_{11} + S_{22} + S_{33}) - 4(S_{12} + S_{13} + S_{23}) + 3(S_{44} + S_{55} + S_{66})} \quad (10)$$

where S_{ij} are the elastic deformation constants.

From the mathematical expressions for the above coefficients, from 3 to 7, the variations of B and G as a function of pressure are illustrated in Figure 7.

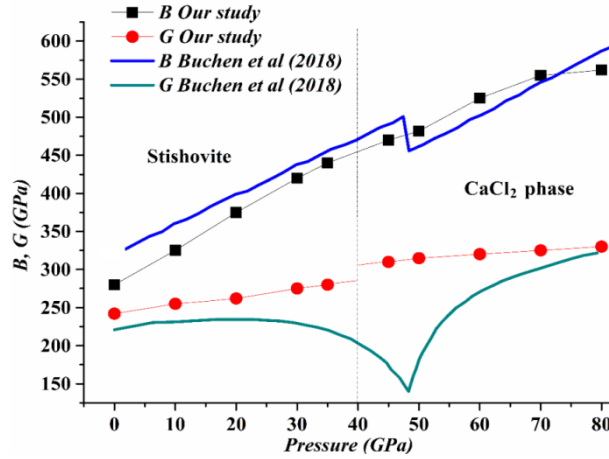


Fig. 7. The variation of bulk modulus, B , and shear modulus, G , as a function of pressure for SiO_2 for stishovite (0 to 40 GPa) and CaCl_2 -type (40 to 80 GPa) compared to [22].

From the obtained results, for both modulus, we deduced a very little change around phase transition zone principally at 35 GPa compared to the results of [22] using synchrotron X-ray diffraction, where a large difference is obtained. In stishovite phase, B increases with pressure up to 35 GPa then the augmentation becomes more through CaCl_2 -type phase transition. The same observation occurred to G , but the increase is smaller compared to B values. The instability of B and G observed around 40 GPa, and due to the transition from the tetragonal phase (stishovite) to the orthorhombic phase of CaCl_2 -type phase. We believe that the constant B values in the range 70-80 GPa amounts to another phase transition from the orthorhombic CaCl_2 -type structure to the seifertite structure of SiO_2 according to [11] and [17].

The isotropic B and G of stishovite at 0 GPa pressure calculated from the elastic coefficients are in agreement with the experimental data of [29] and the results of [28] as shown in Table 2 summarized by [9] and [11]. From this comparison, it is clear that our obtained B is the smallest (284 GPa), and G has a high value just after thus of [33] (241 GPa).

Table 2. Comparison between B and G moduli in GPa (abbreviations are as in Table1).

	B	G
GGA (this study)	284	241
LAWPP [11]	310	232
LAPW [15]	324	
Exp [16]	316	226
BKS potential [23]	463.8	268.5
ab initio, LDA-PWPP [24]	336.1	224.6
KA pseudopotential [26]	314.7	219
FHI pseudopotential [26]	308.7	224

4. Conclusion

In the present study, we defined the elastic properties of SiO_2 nanostructure at from 0 to 80 GPa pressure domain. We found a phase transition of SiO_2 at a pressure of 40 GPa where it changes from a stishovite structure to the CaCl_2 -type one. The pressure dependence of density, elastic constants, bulk modulus, and shear modulus were computed.

From our study, the stishovite takes on a undetectable volume variation. The density ρ of stishovite has an average value relative to the previous studies. As it has been confirmed, it increases proportionally with pressure without any jump indicating that the stishovite- CaCl_2 -type phase transition cannot be considered as a seismological discontinuity despite this pressure

boundary jumps are observed in the elastic constants at 40 GPa. On the other hand, the bulk modulus of stishovite is considerable.

The method followed in the present study allows us to study a different phases of SiO₂. This method will enable us to study the other oxides by determining their elastic properties.

References

- [1] Condie K.C., Academic Press, 2011.
- [2] Stishov S.M., Popova S.V., 10, 839 - 937, 1961; <https://doi.org/10.4269/ajtmh.1961.10.839>
- [3] Kayama, M., Nagaoka, H.; and TNiihara, T. Minerals 2018, 8, 267; <https://doi.org/10.3390/min8070267>
- [4] Tomioka, N.; Miyahara, M. Planet. Sci. 2017, 52, 2017 ; <https://doi.org/10.1111/maps.12902>
- [5] Chao E., Fahey J., Milton D.J., J. Geophys., 67, 419 - 421, 1962 ; <https://doi.org/10.1029/JZ067i001p00419>
- [6] Akaogi M. and Navrotsky A. Physics of the Earth and Planetary Interiors. Volume 36, Issue 2, Pages 124-134, 1984 ; [https://doi.org/10.1016/0031-9201\(84\)90013-X](https://doi.org/10.1016/0031-9201(84)90013-X)
- [7] Karki, B.B., Stixrude L., CrainJ., Geophysical Research Letters, ,24, 3269-3272, 1997 ; <https://doi.org/10.1029/97GL53196>
- [8] Tsuchiya T., Caracas R., Tsuchiya J., Geophysical Research Letters, 31, L11610, 2004 ; <https://doi.org/10.1029/2004GL019649>
- [9] Karki B.B., Stixrude L., Wentzcovitch R.M., , Rev Geophys., 39:507-534, 2001 ; <https://doi.org/10.1029/2000RG000088>
- [10] Yang, R., Wu, Z. Earth and Planetary Science Letters 404 14-21, 2014 ; <https://doi.org/10.1016/j.epsl.2014.07.020>
- [11] Blase, X. <https://hal.archives-ouvertes.fr/hal-03070870>.
- [12] Pabst W. and Gregorová E., Ceramics - Silikáty 57 (3) 167-184, 2013.
- [13] Hohenberg P., and Kohn W., Phys. Rev. 136, B864, 1964 ; <https://doi.org/10.1103/PhysRev.136.B864>
- [14] Segall M.D., Lindan P.J.D., Probert M.J., Pickard C.J., Hasnip P.J., Clark S.J., Payne M.C., J. Phys.,Lett, 14, p 2717, 2002 ; <https://doi.org/10.1088/0953-8984/14/11/301>
- [15] Clark Stewart J., Segall Matthew D., Pickard Chris J., Hasnip Phil J., Probert Matt I. J., Keith Refson and Payne Mike C. ; <https://doi.org/10.1524/zkri.220.5.567.65075>
- [16] Payne J.W.,Bettman J.R., Schkade D.A., Fuqua School of Busi, 1998.
- [17] Hemley R.J., Mao H.K., Gramsch S.A., Mineralogical Magazine, 64(2), p 157, 2000 ; <https://doi.org/10.1180/002646100549265>
- [18] Kathleen J.K., Ronald E., Cohen, Russell J.H., Kwang M., Letters to nature, 374, 1995.
- [19] Aramberri, H., Rurali, R., and Íñiguez, J. Physical Review B 96, 195201, 2017 ; <https://doi.org/10.1103/PhysRevB.96.195201>
- [20] Fischer, R. A., Campbe, A. J., Chidester, B. A., Reaman, D. M. Thompson, E. C. Prakapenka, P., and, Smith, J. S. American Mineralogist, Volume 103, pages 792-802, 2018 ; <https://doi.org/10.2138/am-2018-6267>
- [21] Andrault, D., Fiquet, G., Guyot, F., Hanfland, M., Science, 282, 720 - 724, 1998 ; <https://doi.org/10.1126/science.282.5389.720>
- [22] Buchen, J., Marquardt, H., Schulze, K., Speziale, S., Ballaran, T. B., Nishiyama, N., and Hanfland, M. Journal of Geophysical Research: Solid Earth 10.1029/JB015835, 2018.
- [23] Driver, K.P., Cohen, R.E., Wu, Z., Militzer, B., López Ríos, P., Towler, M.D., Needs, R.J., and Wilkins, J.W. Proceedings of the National Academy of Sciences, 107, 9519-9524, 2010 ; <https://doi.org/10.1073/pnas.0912130107>
- [24] Wang, F., Tange, Y., Irifune, T., and Funakoshi, K.-i. Journal of Geophysical Research, 117, B06209, 2012 ; <https://doi.org/10.1029/2011JB009100>

- [25] Sun, N., Shi W., Mao, Z., Zhou, C., and Prakapenka, V, B., Journal of Geophysical Research: Solid Earth 10.1029/JB017853, 2019.
- [26] Anatoly, B.B., Leonid S.D., Natalya A.D., American Mineralogist, 82, p 1043, 1997.
- [27] Schreiber, E. L. Anderson, O. Soga, N., Elastic Constants and Their Measurement, McGraw-Hill, New York, 1973.
- [28] Cohen, R.E., Am. Mineral., Lett., 76, p 733, 1991.
- [29] Weidner, D. J., and M. T. Vaughan, J. Geophysical Research. Lett., 87, p 9349, 1982 ; <https://doi.org/10.1029/JB087iB11p09349>
- [30] Voigt W., Lehrbuch der Kristallphysik, Taubner, Leipzig, 1928.
- [31] Reuss A., Angew Z., Math. Mech. 9, p 49, 1929 ; <https://doi.org/10.1002/zamm.19290090104>
- [32] Nye J.F., Oxford Science Publications, Oxford, England, 1957.
- [33] Tse J.S., Klug D.D., J. Chem. Phys., 95:9176-9185, 1991 ; <https://doi.org/10.1063/1.461198>